부착되지 않은 텐돈을 갖는 PS 콘크리트 연속부재의 해석적 연구

Analysis of Prestressed Concrete Continuous Members with Unbonded Tendons

문정호* 이리형**
Moon, Jeong-Ho Lee, Li-Hyung

요 약

본 연구에서는 부착되지 않은 텐돈을 갖는 PS 콘크리트 구조체에 대한 해석적 연구가 진행되었는데 해석결과는 기존의 실험결과들과 비교되었다. 기존의 실험 결과들로 부터 하중변위 관계, 구조체의 파괴시 텐돈응력에 대한 설계식, 기존의 보통 철근량의 효과, 부재길이에 대한 부재두께의 효과, 하중의 종류에 따른 영향 등을 해석적 연구와 병행하여 분석하였다. 총 12개의 실험결과가 분석되었는데, 그중 6개는 2 스팬 연속보이며, 나머지 6개는 3 스팬 연속 슬래브였다. 해석 결과는 실험결과와 잘 일치함을 보여 주었으며, 구조체의 파괴시 텐돈의 응력은 기존의 보통 철근의 효과, 하중의 종류, 하중의 패턴, 텐돈의 형상 등에 따라 많은 영향을 받는 것으로 나타났다.

Abstract

The prestressed concrete continuous members with unbonded tendons were investigated while comparing the experimental data with the analytical results. The comparison was carried out with the program TAPS which can take into account the unbonded tendon effects. The subjects that were interested included the load-deflection response, the design equations for the tendon stress at failure, the effects of bonded reinforcements, the effects of span-depth ratio, the effects of loading type. In this paper, continuous prestressed concrete members with unbonded tendons were investigated. Of twelve tests with continuous members, six were two-span beams and six were three span one-way slabs. Analytical results were compared favorably with experimental data and disclosed that the tendon stress at flexural failure is the function of the amount of bonded reinforcements, the loading types and patterns, and the tendon profile.

Keywords : unbonded tendon, continuous member, load-deflection response, tendon stress at failure, bonded reinforcement, span-depth ratio, loading type, pattern loading.

* 한양대 초대형구조시스템 연구센터 연구조교수
** 정회원, 한양대학교 건축공학과 교수

• 본 논문에 대한 토의를 1996년 2월 28일까지 학회로 보내주시면 1996년 4월호에 토의회답을 게재하겠습니다.

1. Introduction

The members with unbonded tendons are not yet fully investigated although the unbonded tendons have been applied for long time due to its possibility of economic, simple, fast construction as well as easy replacement of defective tendons. The strength of member is affected by the incompatibility of tendons with concrete. However, the unbondness cannot be accounted for only by the cross-sectional analysis at a few critical locations. No code equations, currently, take into account the effects of unbonded tendons. Although a few of research efforts were undertaken by some authors,[1,2,3] most of them were devoted to developing analytical tools and design equations for simply supported members. Thus, the main purpose of this paper is to study the unbonded tendon effects in continuous members.

The program TAPS[4] can take into account the effects of unbonded tendons. With the program TAPS, experimental data in the literature have been examined to investigate the behavior of prestressed concrete member with unbonded tendons. Major objectives were the followings: (1) the examination of the load-deflection response; (2) the comparison of the tendon stress at flexural failure with design equations; (3) the investigation of the effects of bonded unstressed reinforcements; (4) the examination of the effects of span-depth ratio; (5) the investigation of the effects of pattern loading and cyclic loading.

A total of twelve tests of continuous members with unbonded tendons were investigated with the program TAPS. Of twelve tests with continuous members, six were Burns, Helwig, and Tsujimoto's two-span beams[5] and six were Burns, Charney, and Vine's three span one-way slabs.[6] The tendon stress at flexural failure were compared with the ACI Code (Eq. 1) and Naaman and Akahaili's equation[2,3] (NA, Eq. 2) as well as the program TAPS.

$$f_{ps} = f_{se} + 10000 + \frac{f'_c}{k\rho_p} \qquad (1)$$

where = effective stress in prestressed reinforcement; is the ratio of prestressed reinforcements; k is 100 for the span-to-depth ratio of 35 or less, 300 for the span-to-depth ratio greater than 35.

$$f_{ps} = f_{se} + \Omega_u\, 0.003E_{ps}\left[\frac{d_{ps}}{c} - 1\right]\left[\frac{L_1}{L_2}\right] \le 0.94f_{py} \qquad (2)$$

where Ω_u is the coefficient of loading type; E_{ps} is the elastic modulus of tendon; d_{ps} is distance from extreme compression fiber to tendon; c is distance from extreme compression fiber to zero stress point; are length of loaded span and length of tendon, respectively.

2. Analytical study

2.1 Burns, Helwig, and Tsujimoto's beams (BHTs)

Prestressed concrete members with unbonded tendons have been tested for more than three decades. However, only a few of them were continuous members and none of them were tested under cyclic loads. The stress change in unbonded tendons depends upon not only the local deformation but also the whole member deformation. Therefore, a study was needed for continuous members with unbonded tendons under repetitious application of cyclic loads. Burns, Helwig, and Tsujimoto conducted a test program with two continuous beams under cyclic loads.

The beams were called the shallow beam and the deep beam depending on their heights of 14 in and 22 in, respectively. They were continuous over two 25 ft spans and posttensioned with three unbonded 1/2 in diameter prestressed strands to the initial stress of approximately 0.75. Bonded rebars were also provided to satisfy the ACI Code requirement of minimum bonded reinforcements. Each beam was tested under the various sequences of cyclic loading which were ranged from the cracking load to the ultimate load. The number of loading stages was eighteen for the shallow beam and twenty four for the deep beam. The loads were applied to produce maximum moments at various locations at a given level of load. For analytical purposes, it was assumed that each loading stage was applied to the virgin specimen which was not affected by any prior loading histories. Each loading stage was, then, given an individual name and considered as an individual test. In this study, the tests subjected to the overload or the ultimate load were chosen to examine the inelastic behavior. The stages selected were a total of six tests that consisted of three for each beam. The analytical loading sequences were not identical with the experimental procedures because the actual procedures were mixed each other during the tests. The names of the tests were designated by two letters with the first letter for the beam heights (S for shallow and D for deep beams) and the second one for the loading stages (N for north, S for south, and B for both span loadings, see Table 1).

The measured load-deflection responses were compared with the analytical solutions. The effect of prior loading histories was simulated by applying one cycle of overload to produce cracks at critical locations. The comparisons of load-deflection response and the load-stress increase relation are shown in Fig. 1, Fig.2. The actual tests of BHT.SN and BHT.DB were not loaded up to their peak strengths to allow for the further stages of load. However, all the other tests were conducted to approach their failure strengths at critical sections. The predicted load-deflection responses agreed well with the experimental curves. A difference was found in the residual deflection after the applied load was removed completely. The analytical deflection recovered completely while residual deflection remained experimentally. The unloading and reloading paths of the analytical curves were almost identical to the test curve when the levels of applied load were not significant. As the deformation increased, however, the energy dissipation deteriorated the reloading stiffness but the strength of the beams were not affected by the energy dissipation. The early strengths of the deep beam were predicted slightly less

Table 1 Details of BHTs

name	h (in)	f'_c (ksi)	A_{ps} (in^2)	f_{se} (ksi)	ρ_{ps}	A_s (in^2)	f_y (ksi)	f_u (ksi)	ρ_s	ω_e
BHT.SS	14	5.976	0.459	177.0	0.003	0.40	66	106	0.003	0.136
BHT.SN	14	5.976	0.459	177.0	0.003	0.40	66	106	0.003	0.136
BHT.SB	14	5.976	0.459	177.0	0.003	0.40	66	106	0.003	0.079
BHT.DS	22	5.763	0.459	186.9	0.002	0.62	73	110	0.003	0.172
BHT.DN	22	5.763	0.459	186.9	0.002	0.62	73	110	0.003	0.172
BHT.DB	22	5.763	0.459	186.9	0.002	0.62	73	110	0.003	0.172

Note : $\omega_e = \rho_s \frac{f_y}{f'_c} + \rho_{ps} \frac{f_{se}}{f'_c}$, 1 in = 25.4 mm, 1 ksi = 6.89 MPa

than the test strengths. But the analytical strengths increased steadily with following the experimental curves. The analytical tendon stresses were usually less than the initial effective stresses after the removal of applied load. But it was apparent that the shapes of stress increase curves were similar to the deflection curves.

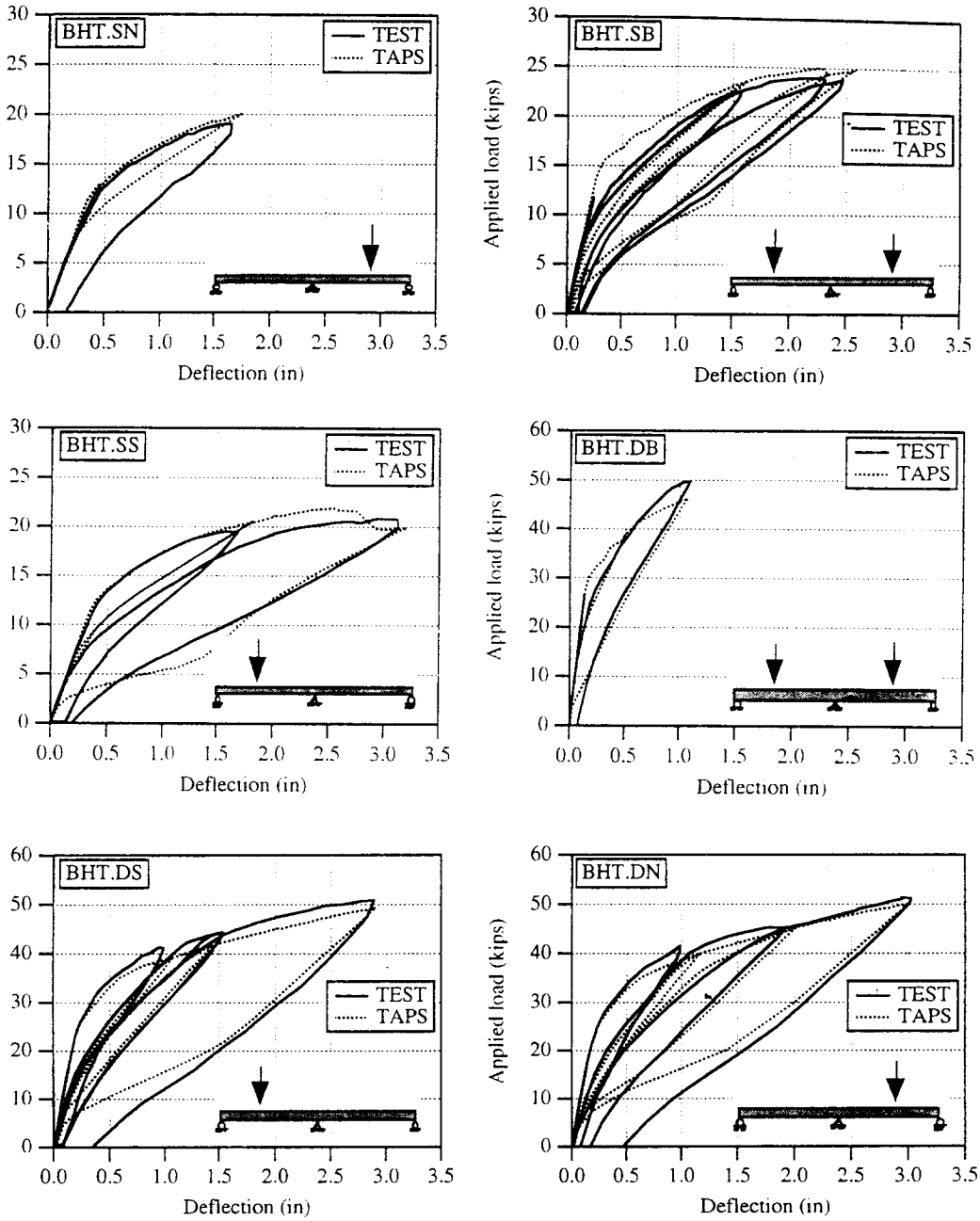

Fig.1 Comparison of deflections with Burns, Helwig, and Tsujimoto's tests(1 kip=4.448 KN, 1 in=25.4 mm)

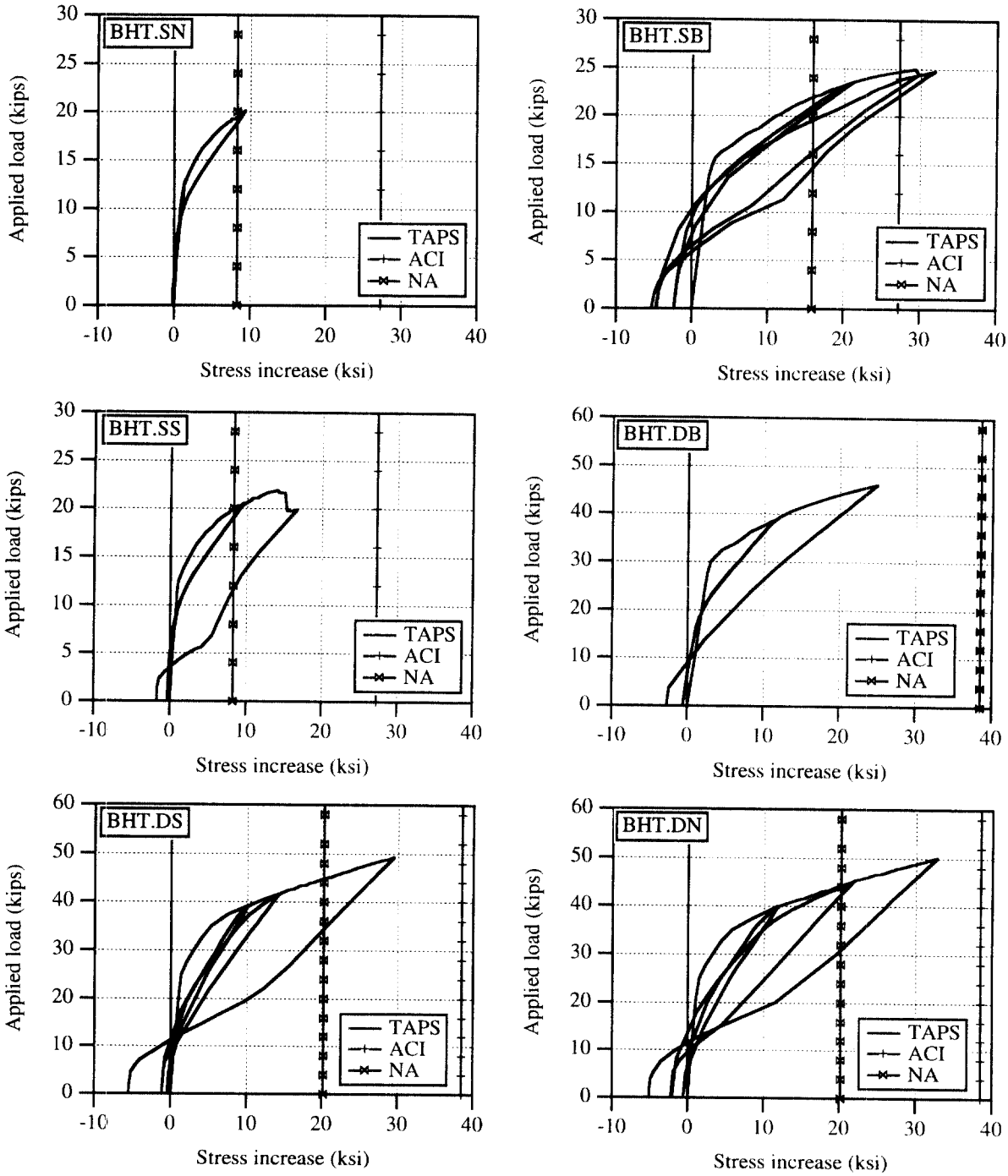

Fig.2 Comparison of tendon stresses with Burns, Helwig, and Tsujimoto's tests(1 kip=4.448 KN, 1 ksi=6.89 MPa)

2.2 Burns, Charney, and Vines' slabs (BCVs)

At the University of Texas at Austin, a test program was carried out to understand the behavior of partially prestressed concrete slab with unbonded tendons. Burns, Charney, and Vines designed two prototype slabs with three continuous spans (slab A and slab B). The

actual dimensions of prototype slabs were then reduced to half-scale models for the experimental purpose. The objectives of the tests were to examine: (1) the effects of cracking on the partially prestressed concrete slabs; (2) the effects of bonded unstressed reinforcements; (3) the change of tendon stress up to the ultimate strength of slab. The effects of cracking were examined by limiting the allowable tensile stress to 6 (psi) for the slab A and 9 (psi) for the slab B. Bonded reinforcements were supplied to control cracking although the amount was less than that of the ACI requirement for the slab A. The reinforcement provided was 0.12 percent of cross-sectional area for the slab A and 0.23 percent for the slab B. The tendon stresses were measured along the tendon length while the pattern loadings were imposed on the slabs to produce maximum stress at various locations.

The physical dimensions were identical for both slabs which were made with three continuous spans of 10 ft each and a uniform thickness of average 2.94 in. The unbonded tendons were 1/4 in diameter single wire with a measured strength of 240 ksi and a specified strength at 1% elongation of 213 ksi. The tendons were stressed from both directions in such a way that part of the tendons were tensioned from the left end and the remainder were tensioned from the right end. Each slab was subjected to a total of ten patterns of various loadings among which the last three tests were intended to investigate the ultimate load behavior. They were named as BCV.108, 109, 110 for slab A and BCV.208, 209, 210 for slab B (see Table 2). It was found that the slabs were not provided with a proper reinforcing details since the bonded flexural reinforcements were terminated in tension zone. The ACI Code requires that the reinforcements extend a certain distance beyond the point at which it is no longer required to resist flexure. Furthermore, span B of both slabs was not provided with any of the top reinforcements which may be required for the pattern loadings for test BCV.108 and BCV.208. Fig.3, 4 show the load-deflection and the load-stress increase relations.

Each test was analyzed as an individual test independent of prior load histories except BCV.110 and BCV.210. However, one cycle of loading and unloading was applied to produce cracks at critical sections since the slabs had been subjected to various types of previous loads. Each test was also analyzed as if it were erected with a sufficient development length of bonded bars in order to investigate any information lost due to the improper details. In this study, the analytical solutions of actual tests will be represented by the name of TAPS.1 while the analytical solutions of the

Table 2 Details of BCVs

name	f'_c (ksi)	A_{ps} (in^2)	f_{se} (ksi)	A_s (in^2)	f_y (ksi)	ρ_{ps}	ρ_s	ω_e
BCV.108	4.70	0.196	141.5	0.196	65	0.0016	0.0016	0.0696
BCV.109	4.70	0.196	141.5	0.196	65	0.0016	0.0016	0.0696
BCV.110	4.70	0.196	141.5	0.000	65	0.0016	0.0000	0.0477
BCV.208	5.15	0.147	146.0	0.343	65	0.0012	0.0028	0.0687
BCV.209	5.15	0.147	146.0	0.343	65	0.0012	0.0028	0.0687
BCV.210	5.15	0.147	146.0	0.098	65	0.0012	0.0008	0.0437

Note : $\omega_e = \rho_s \frac{f_y}{f'_c} + \rho_{ps} \frac{f_{se}}{f'_c}$, 1 in = 25.4 mm, 1 ksi = 6.89 MPa

slabs with extended reinforcements will be called TAPS.2.

Test BCV.108 was loaded to produce failures in span A and C while span B was subjected to 1.4 times of dead load. As the applied load increased, numerous cracks were formed in positive moment regions in span. At the load level of 135 psf, however, the deflection increased with no increase of load but no signs of compression failure were detected. The analytical curvature variations showed that the inelastic deformations initiated at the desired locations of maximum positive moment region in span A and span C. The load-deflection curve illustrates that the theoretical cracks were formed at the bar-cutoff points of span A and C at deflection of about 1.69 in. Up to this level of load, the improper details of reinforcing steels caused no significant differences in the load deflection curve. The cracks at the bar-cutoff point, however, induced a reduction of strength of test BCV.108. A slight drop of strength at the deflection of 1.25 in was produced by the cracking at the midspan of span B since the slab was not provided with any negative reinforcements in this region.

Test BCV.109 was carried out to produce a maximum positive moment in span A and a maximum negative moment over support 2. Although critical cracks were also formed at the bar-cutoff points, they were proceeded by the formation of significant flexural cracks in the negative moment region over support 2. Theoretically, the first plastic hinge was developed at the maximum negative moment region. However, the second plastic hinge was formed at the maximum positive moment region at which bonded reinforvements are not being cut off. Based on the comparison of load-deflection curves, it can be considered that the capacity of test BCV.109 was not damaged significantly by the improper reinforcing details. Since the first plastic hinge was formed at the desired location which had enough bonded reinforcement, relatively higher strength was obtained experimentally and analytically. The load-deflection curves were predicted well regardless of the reinforcing details. The stress in tendon, however, was underestimated and the test curve deviated from the analytical curve at an early stage of load.

Although the previous load history for test BCV.108 and test BCV.109 could be simulated simply by applying a cycle of loading and unloading, test BCV.110 cannot be analyzed accurately without considering the previous load history. Since a plastic hinge was already developed over support 2 during test BCV.109, the analysis of test BCV.110 should begin from the point at which the plastic hinge was formed from the previous tests. After the plastic hinge was formed over the support 2, the applied load of test BCV.109 was removed and the load for test BCV.110 was applied. A theoretical plastic hinge during test BCV.110 was developed at approximately 0.45L from support 2. The eventual failure was reached by the formation of three plastic hinges. But the test showed that only a large crack was developed at the midspan of span B. It was attributed mostly to the fact that no bonded reinforcements were provided at the midspan region of the center span. Therefore, it is considered that a premature failure occurred for test BCV.110. However, the theoretical load-deflection showed a steady increase of strength since the program TAPS could not capture such an undesirable failure mode correctly. The failure strength of test BCV.110 was governed by an arching action rather than the flexural mode.

The slab B was designed with the higher lev

el of allowable tensile stress than the ACI Code requirement. The reinforcement provided for the slab B was 75 percent for the prestressing steel and 175 percent for the unstressed bonded steels when they were compared with slab A. Since the cracking was expected in an early stage of load due to its lower amount of prestressing steels, the tension zone without any bonded reinforcement would be more critical than the slab B. Test BCV.208 was loaded on spans A and C while maintaining 1.4 times of dead load on span B. The strength of test BCV.208 was governed by the formation of large flexural cracks in the positive moment regions where the bonded reinforcements had been cut off. Those cracks developed at about 4 ft from support 2 while the theoretical failure crack was formed at about 3.9 ft from support 3. Therefore, it can be said that those two locations are identical in view of structural behavior. The load-deflection curve shows that the applied load was reduced suddenly from the level of 150 psf at around 0.88 in deflection and stabilized at the load of experimental failure load. It is considered that the failure strength of test BCV.208 was decreased by its lower cracking strength. This is why the slab failed at the lower load of 120 psf than test BCV.108 of 135 psf. The load-carrying capacity of slab was increased with the extension of positive reinforcement. A slight decrease of strength at the deflection of 1.4 in was due to the cracking at the top of span B. As mentioned, no negative reinforcements was provided to prevent the cracks in the span B.

For test BCV.209, spans B and C were loaded while maintaining 1.4 times of dead load for span A. The test was intended to examine the ultimate load capacity of the slab for the loadings which produced the maximum negative moment over support 3 and a high positive moment in span C. At the load level of about 120 psf, cracks over support 3 and in span C increased in depth. A large and critical crack was formed 2 ft from support 4 when the applied load approached 150 psf. Test BCV.209 was stopped at the deflection of 1.2 in with the load level of 145 psf. The theoretical failure load was reached when a crack was formed at the cutoff point located 4 ft from support 3. After a sudden drop of load, the load-deflection curve became stable with an increase of deflection. The comparison of load-deflection curves illustrates that test BCV.209 responded with a good flexural mode until the critical crack was formed in span C. Since test BCV. 209 failed after large deformations over support 3, the actual strength of the slab could reach close to the theoretical strength before the critical crack was formed.

During test BCV.210, span B was loaded to failure while span A and span C remained at 4 times dead load. The reinforcement provided for span B was one half that of span A or C. At the applied load level of 120 psf, a large crack was detected at midspan. As the load increased, the crack grew in width and depth and the failure occurred at approximately 160 psf. The experimental load-deflection curve showed a bilinear relation as shown in Fig. 4. Failure is attributed to the fact that the amount of bonded reinforcement was not enough to distribute the concentrated concrete strain effectively over adjacent sections. Although the analytical solution showed that the second and third plastic hinges were formed over support 2 and 3, such hinges were not detected during test BCV.210. Therefore, it is considered that a premature failure occurred in test BCV.210.

The structural behavior is affected by various sources such as the loading pattern, the

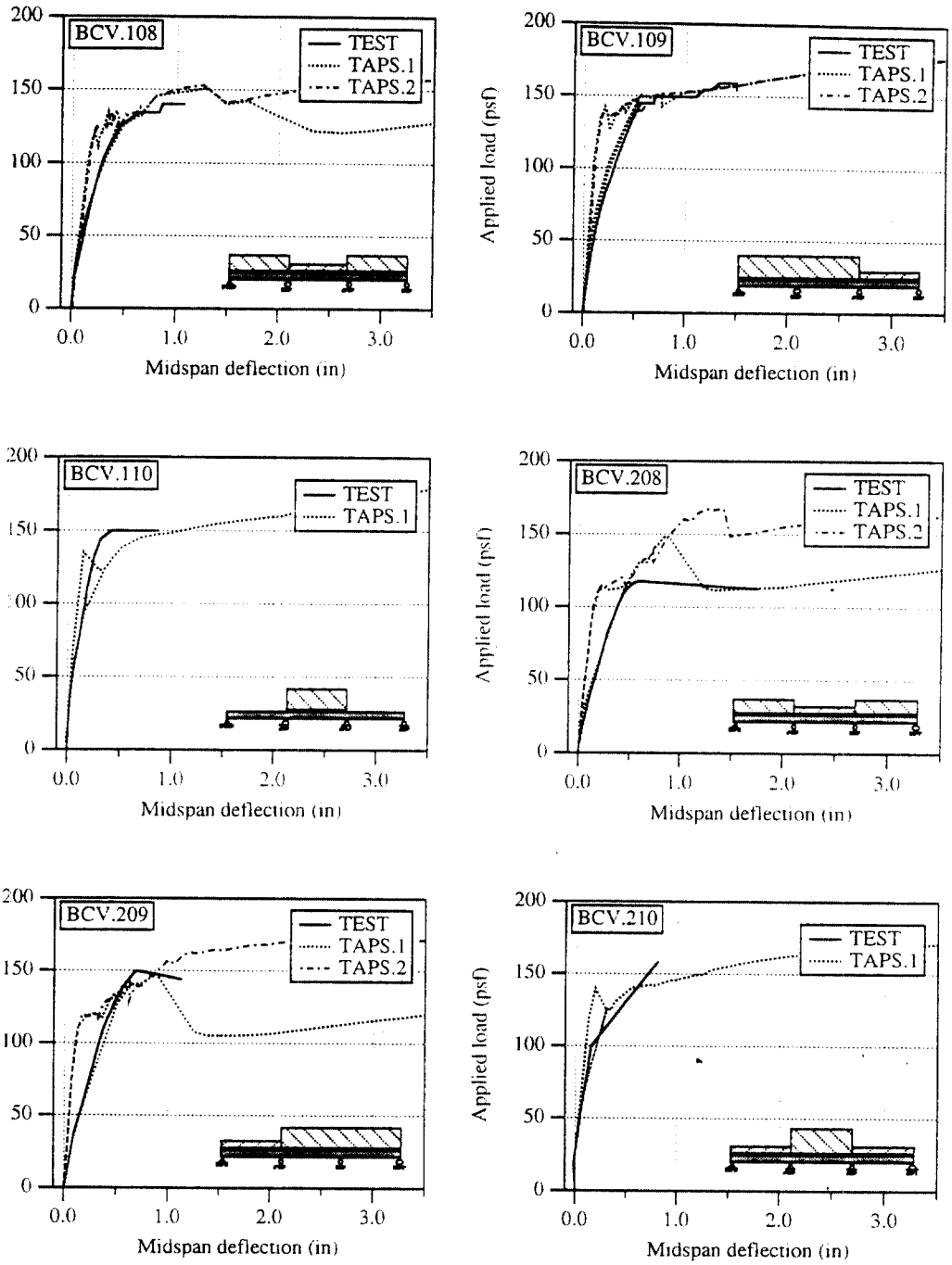

Fig.3 Comparison of deflections with Burns, Charney, and Vines' tests(1 psf=47.9 Pa, 1 in=25.4 mm)

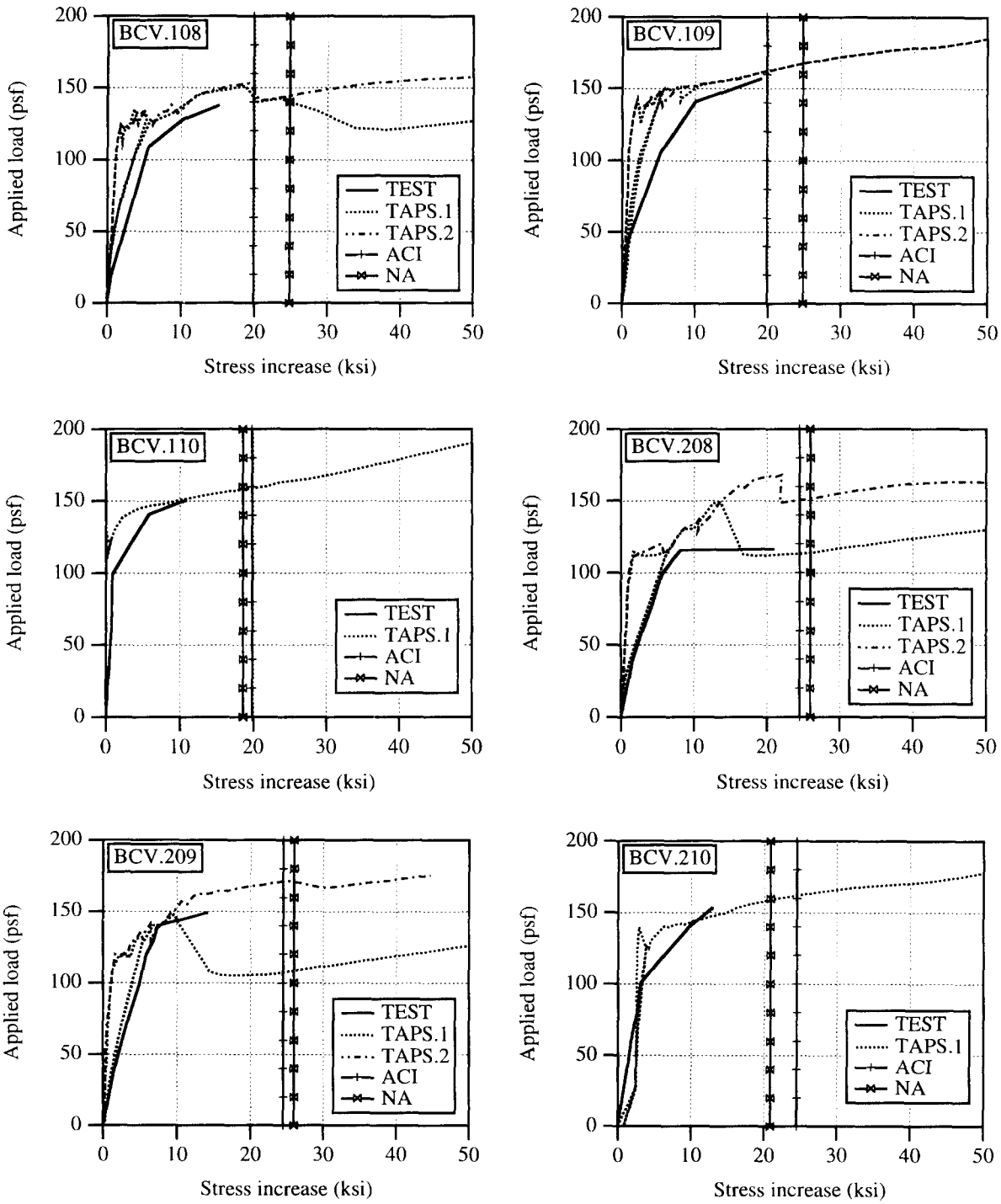

Fig.4 Stress increases of Burns, Charney, and Vines' tes ts(1 psf=47.9 Pa, ksi=6.89 MPa)

loading sequence and the reinforcing ratio. All the theoretical strength except tests BCV.109 and BCV.209 reached by the formation of first plastic hinge. Their failures were attributed to a few large cracks at the cutoff point where the bonded reinforcements were not supplied to control the crack. Those failure modes can be classified as the undesirable modes since those slabs should have developed additional plastic hinges before their failures. Test 109 and test BCV.209 were also failed with the undesirable mode. However, the nonlinear deformation had preceded extensively before the undesirable cracks formed at the critical locations. The nonlinear deformation occurred in a ductile manner over support 2 for test BCV. 109 and support 3 for test BCV.209 where the bonded reinforcement was provided with an enough length to control flexural cracks. Since both tests failed eventually as a result of the undesirable cracks, it can be concluded any test whichever has a higher cracking strength, like test BCV.109, behaved in a more ductile manner. The comparison of load-deflection curves proved that test BCV.109 failed in a ductile mode and its deflection could increase whil e forming plastic hinges if the bonded steel had been extended sufficiently.

3. Tendon stress at flexural failure

The tendon stresses were not measured during the tests of BHTs. Thus, the measured end forces were compared with the analytical solutions in Fig. 5. The actual tendon stress at a critical location would lie approximately between the stresses of jacking and holding ends since tendons are unbonded. The tendon stresses at failure were also computed with the ACI and NA's equations. Since BHT.SN and BHT.DB were not loaded up to their maximum capacity, the observed stresses were less than the actual peak strengths. Fig. 5 shows that TAPS underestimate the tendon stress as the beam depth became higher. The predicted stress increases of the ACI Code were as twice as the experimental stress increases for test BCV.110 and BCV.210 that were loaded only on the center span. A similar trend was found for the Naaman and Akahaili's equation. Since test BCV.109 and BCV.209 developed a plastic hinge at the desired locations before the formation of cracks at the bar-cutoff points, the predicted stress were closer to the actual stress. The effects of pattern loading were described well with the program TAPS while predicting relatively smaller increases in tendon stress for tests BCV.110 and BCV.210. The analytical studies proved that the unbonded tendon stress at flexural failure is the function of the amount of bonded reinforcements, the loading types and patterns, and the tendon profile. However, the ACI equation does not take into account those effects for the flexural design.

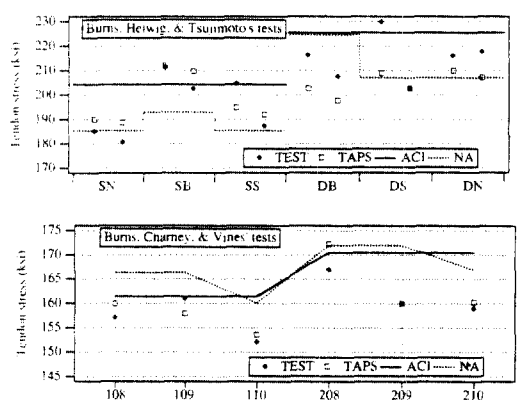

Fig.5 Comparison of tendon stresses(1 ksi=6.89 MPa)

4. Conclusion

Analtical studies for prestressed concrete member with unbonded tendons were carried

out and compared favorably with the experimental data. A large number of tests on continuous prestressed concrete members were examined with the program TAPS and the following conclusions were obtained.

1. The cyclic load-deflection and load-stress increase curves for BHTs were predicted close to the measured curves. However, no residual deflections were predicted at the removal of applied load although certain levels of residual deflection were observed from the tests.
2. The analytical studies on BCVs indicated that the test slabs failed by the improper reinforcing details of bonded steel. The analytical strengths of tests were increased with the assumed reinforcing details in which the positive reinforcement was extended to supports.
3. The load-deflection relationships of BCVs were predicted well while the load vs. tendon stress curves were slightly underestimated by the analyses.
4. It was found that BCV.108, 109, and 110 were less affected by the reinforcing details since they were designed to have higher cracking strengths than BCV.208, 209, and 210.
5. Theoretically, the test of BCV.109 is considered that it failed in the most ductile manner compared with other tests since it had a higher cracking strength and the fir st plastic hinge was developed at the desirable location.
6. The effects of pattern loading on the tendon stress at failure were predicted well for BCV.110 and 210. The stress increases in the tendon were very small since only one span was loaded among the total of three spans.
7. The numerical studies of unbonded members proved that the ACI Code should take into account the effects of bonded reinforcement, the loading conditions, and the loading pattern for the computation of the unbonded tendon stress at flexural failure.

References

1. Harajili, M. H., "Effect of Span-Depth Ratio on the Ultimate Steel Stress in Unbonded Prestressed Concrete Members," ACI Structural Journal, Vol.87, No.3, May-Jun., pp. 305-312.
2. Naaman, A. E., Alkhairi, F. M. (1991). "Stress at Ultimate in Unbonded Post-Tensioned Tendons: Part 1 - Evaluation of the State-of-the-Art," ACI Structural Journal, Vol.88, 5, Sept.-Oct., pp.641-650.
3. Naaman, A. E., Alkhairi, F. M. (1991). "Stress at Ultimate in Unbonded Post-Tensioned Tendons: Part 2 - Proposed Methodology," ACI Structural Journal, Vol.88, No.6, Nov. -Dec., pp.683-692.
4. "Analytical Method of Prestressed Concrete Members with Unbonded Tendons," being reviewed for possible publication.
5. Burns, N. H., Helwig, Todd, and Tsujimoto, Tetsuya (1991). "Effective Prestressed Force in Continuous Post-Tensioned Beams with Unbonded tendons," ACI Structural Journal, Vol.88, No.1, Jan.-Feb., pp.84-90.
6. Burns, N. H., Charney, F. A., and Vines, W. R. (1978). "Tests of One-way Post-Tensioned Slabs with Unbonded Tendons," PCI Journal, Vol.23, No.5, Sept.-Oct., pp.66-83.
7. ACI-ASCE Committee 423 (1989), "Recommendations for Concrete Members Prestressed with Unbonded Tendons," ACI Structural Journal, May-June.

(접수일자 : 1995. 10. 4)